Sugar-Based Polyamides: Self-Organization in Strong Polar Organic Solvents

ARTICLE *in* BIOMACROMOLECULES · AUGUST 2015

Impact Factor: 5.75 · DOI: 10.1021/acs.biomac.5b00977

Article

pubs.acs.org/Biomac

Sugar-Based Polyamides: Self-Organization in Strong Polar Organic Solvents

Cornelia Rosu,[*,†,‡,§] Paul S. Russo,[†,‡,§,∥] William H. Daly,[‡] Rafael Cueto,[‡] John A. Pople,[⊥] Roger A. Laine,[#] and Ioan I. Negulescu[*,‡,○]

[†]School of Materials Science and Engineering, [∥]School of Chemistry and Biochemistry, and [§]Georgia Tech Polymer Network, GTPN, Georgia Institute of Technology, Atlanta, Georgia 30332, United States

[‡]Department of Chemistry and Macromolecular Studies Group, [#]Department of Biological Sciences, and [○]Department of Textiles, Apparel Design and Merchandising and Agricultural Center, Louisiana State University, Baton Rouge, Louisiana 70803, United States

[⊥]Stanford Synchrotron Radiation Laboratory, Stanford Linear Accelerator Center, Stanford, California 94309, United States

Supporting Information

ABSTRACT: Periodic patterns resembling spirals were observed to form spontaneously upon unassisted cooling of D-glucaric acid- and D-galactaric acid–based polyamide solutions in *N*-methyl-*N*-morpholine oxide (NMMO) monohydrate. Similar observations were made in D-galactaric acid-based polyamide/ionic liquid (IL) solutions. The morphologies were investigated by optical, polarized light and confocal microscopy assays to reveal pattern details. Differential scanning calorimetry was used to monitor solution thermal behavior. Small- and wide-angle X-ray scattering data reflected the complex and heterogeneous nature of the self-organized patterns. Factors such as concentration and temperature were found to influence spiral dimensions and geometry. The distance between rings followed a first-order exponential decay as a function of polymer concentration. Fourier-Transform Infrared Microspectroscopy analysis of spirals pointed to H-bonding between the solvent and the pendant hydroxyl groups of the glucose units from the polymer backbone. Tests on self-organization into spirals of ketal-protected D-galactaric acid polyamides in NMMO monohydrate confirmed the importance of the monosaccharide's pendant free hydroxyl groups on the formation of these patterns. Rheology performed on D-galactaric-based polyamides at high concentration in NMMO monohydrate solution revealed the optimum conditions necessary to process these materials as fibers by spinning. The self-organization of these sugar-based polyamides mimics certain biological materials.

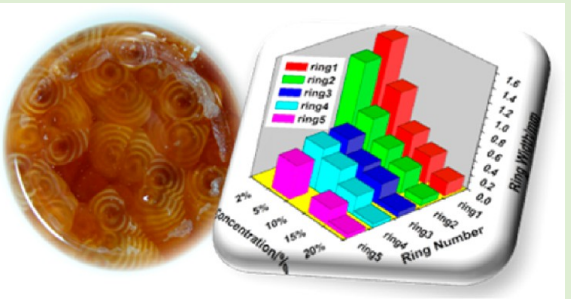

INTRODUCTION

Naturally occurring patterns have attracted extensive interest because of their intriguing beauty. Many self-organized systems often operate far from equilibrium and display a range of morphologies.[1−6] Spherulites are one such morphology, where the term is used to define a spherical shape observed in a wide range of materials, such as pure Se-based metallurgical alloys,[6,7] mineral aggregates and volcanic rocks,[8] simple organic liquids,[9] polymers,[10,11] liquid crystals,[2,3] and some biological structures.[12] Two main categories of spherulites have been recognized based on their nucleation and growth.[5,13] The first refers to the radial growth from a nucleation point with intermittent branching in order to fill the space. Spherulites of the second kind start to grow as threadlike fibers with subsequent formation of new grains in the vicinity of the growth front.[14] Their formation and behavior have been studied in-depth and reviewed.[15,16]

The formation of concentric-ringed (banded) crystalline structures was first reported in polymer thin films by Keith and Padden[17] and by Schuur.[18] The occurrence of the concentric morphologies depends on static heterogeneities, such as impurities, molecular defects, and the polydispersity of the polymers.[19] The growth of these periodic structures can cause the rejection of impurities from the growth front, leading to channel formation.[14]

Certain nonequilibrium morphologies are also known as Liesegang patterns,[20] helicoidal Turing rings,[21] and spiral excitable media.[22−25] Liesegang ring formation requires an initial spatial concentration gradient that initiates a wave of reagents moving through the system. The width of the ring varies in accordance with the distance from the origin to the moving front. The space between bands and their width increases with the number of bands. Similar spiral patterns were obtained by frontal polymerization.[26,27] Many naturally occurring morphologies can be explained using Liesegang structures as a model. Examples range from the structuration of agate gems to the growth of bacterial rings in gallstones.

Received: July 20, 2015
Revised: August 5, 2015

DOI: 10.1021/acs.biomac.5b00977
Biomacromolecules XXXX, XXX, XXX−XXX

Recent studies on banded structures suggest that the formation of spherulites follows a much simpler path, one comparable to Ostwald theory.[28,29] When the polymer diffusion rate is lower than the rate of mass converted to crystals, a depletion zone occurs near the growing crystal that favors the continuous flow of polymer chains to that zone.[30] Furthermore, if the polymer has a high polydispersity, fractionation can result. High-molecular-weight polymers diffuse onto the crystal growth surface and crystallize. The low-molecular-weight polymer chains and impurities will be rejected from the growth surface. They diffuse and deposit onto the fold surface of the crystals to minimize interfacial free energy.[30]

Spherulites formed by self-organization from a solution or melt of biobased polymers, in particular, have been of recent interest.[31] Spherulites are high-order molecular assemblies with desirable properties, such as high mechanical strength. One of the most studied systems is based on poly(L-lactide), PLLA, and its derivatives.[32] Liu et al. found that blends of PLLA with poly(ε-caprolactone), PCL, exhibited well-separated crystalline domains.[33] Selective enzymatic degradation with *Pseudomonas lipase* revealed spheres and island-like patterns. Transitions in crystal growth from the melt of poly(*S*-lactide), PLA, obtained from either lactic acid or the cyclic dimer, were followed by Abe et al.[34] PLA films isothermally crystallized below 145 °C to form uniform, two-dimensional spherulites with lamellar texture. Above 150 °C, the crystals had a hexagonal lamellar packing.[34] Recently, Pan et al. investigated the effects of miscible blending on the crystallization kinetics and crystalline structure of PLLA.[35] Blends with poly(D,L-lactide) organized into both irregular and ring-banded spherulites. Banded extinction rings were reported by Teramoto et al. for both pristine PLLA and grafts with cellulose diacetate at different molar substitutions.[36] Ring-banded spherulites of large pitch were grown from films of poly(L-lactic) acid and poly(ethylene oxide) blends.[37] Cellulose, perhaps the most abundant natural polymer on Earth, has the ability to form spherulitic morphologies in various solvents. Banded spherulites were observed in *N*-methyl-*N*-morpholine oxide, sometimes marked by a ringed Maltese cross.[38] Unusual cellulose spherulites were discovered recently in ionic liquids by Ding et al.[39] These morphologies displayed an eye-like region. Upon heating, the areas exhibiting positive birefringence and evolved into thermodynamically stable negative birefringent zones.

This paper reports the formation of self-organizing patterns upon unassisted cooling of solutions of two sugar-based polyamides in strong polar solvents. The polymers were obtained by the condensation of D-glucaric or D-galactaric acid with 1,6-hexamethylenediamine. These macromolecules (Figure S1, Supporting Information) bear a resemblance to nylon-66, but with heavy hydroxyl substitution along the diacid. Special emphasis will be placed on exploring the behavior and phenomenology of the polymers in *N*-methyl-*N*-morpholine oxide monohydrate (NMMO·H_2O) solution because their self-organization resembles closely that observed in natural systems (e.g., agates). H-Bonding between polymer and solvent play a key role in the formation of the patterns. To investigate this aspect, the free hydroxyl groups on the polymer backbone were blocked with ketal moieties.[40] Protection of side chain functional groups inhibited self-organization of polymers.

MATERIALS AND METHODS

Materials. *N*-Methyl-*N*-morpholine oxide monohydrate (50:50), 1-methylimidazole, 1-chlorobutane, anhydrous acetonitrile, anhydrous toluene, anhydrous diethyl ether, and *n*-propyl-gallate, n-PG, were purchased from Sigma-Aldrich (98 or 99% grade purity). All other starting materials were used as received.

Polymer/Solvent Preparation. *D-Glucaric and D-Galactaric Acid-Based Polyamides.* All unprotected D-glucaric acid-based samples were synthesized following the same literature protocol.[41] Protection of pendant hydroxyl groups of galactose residues was achieved by a literature method.[40,42] The structure (Figure S1) and GPC traces (Figure S2) of unprotected polymers are presented in Supporting Information. Both unprotected and protected polymers were characterized and experimental data can be found along with detailed synthetic procedures in published reports by Rosu et al.[40,43] The molecular weight of unprotected D-glucaric acid-based polymer was M = ~2 kDa with a broad PDI, while the bis-ketal-protected D-galactaric acid-based polymer had M = 5.5 kDa and a PDI = 1.5. For further reference, the two unprotected hydroxylated polyamides will be abbreviated as glu-6 and gal-6.

N-Methyl-N-morpholine Oxide Monohydrate, NMMO·H_2O. The monohydrate form has 13.3 wt % H_2O and 86.7 wt % NMMO. In order to achieve this composition, a mixture containing NMMO·H_2O in a mole ratio of 50:50 (128 g, 948.15 mmol), *n*-propyl-gallate, n-PG (0.256 g, 1.2 mmol), and toluene (15.5 mL) was subjected to azeotropic distillation (60−90 °C) until only the monohydrate content of water remained in the system (13.3 ± 1 wt %). The final water percentage was calculated from the difference between the solvent mass, NMMO·H_2O, before and after azeotropic distillation. Upon cooling to room temperature, the amber NMMO monohydrate was sealed in small polyethylene bags and kept in desiccators (see Figure S3, Supporting Information, for FTIR specific signals).

1-Butyl-3-methylimidazolium chloride, BMIMCl. The preparation of BMIMCl followed a known procedure.[44] For details see Figure S4, Supporting Information.

Solution Preparation. *Polymers in NMMO Monohydrate and Ionic Liquids, BMIMCl.* In solution preparation, the amount of solvent, either NMMO·H_2O or BMIMCl, was kept constant (2.0 g; see Table S1, Supporting Information). Typically, the solvent was weighed in 20 mL scintillation vials with a bottom diameter of 25 mm under an inert atmosphere (nitrogen). Then the polymer was added to it. A small amount of *n*-propyl gallate, n-PG (0.2%), was used to prevent solvent oxidation. The n-PG amount was kept constant at 4.0 ± 0.2 mg. The polymer amount was adjusted as a function of the desired final concentration. The vials were placed in a sand bath and heated to 80 °C in the case of NMMO·H_2O solutions until a clear transparent amber-colored solution was obtained. Afterward, the vials were set on the lab bench to cool to room temperature. The thickness of each solution was 7 mm. The BMIMCl solutions were colorless and transparent.

Equipment. *Microscopy.* Optical microscopy was performed using a Nikon-Microphot FXA microscope equipped with a SPOT Advanced color camera (Diagnostic Instruments, Inc.). An Olympus BH2 microscope was used to investigate the spirals under polarized light. This microscope had an Amscope (model MD 1900-CK) camera attached for capturing images. A Leica TCS SP2 confocal microscope operating in reflection mode was used to investigate the surface details of the structures.

Fourier Transform Infrared Microspectroscopy, Micro-FTIR. FTIR measurements were performed at the Infrared Microspectroscopy Beamline, Port 1A, located at the Center for Advanced Microstructures and Devices, CAMD, Louisiana State University, Baton Rouge, LA. See Supporting Information for details.

Thermal Analysis. Differential scanning calorimetry, DSC, was carried out using a 2920 MDSC V2 6A instrument from TA Instruments under nitrogen. The sample weight was in the range of 3−6 mg. The reference consisted of an empty aluminum pan with cover, identical to that used to hold the sample. Thermogravimetric analysis, TGA, was performed on a Mettler 2950 TGA HR V6.1A instrument. The sample mass varied between 2.5 and 24 mg. The scan rate was set at 10 °C min^{-1} under nitrogen. The sample was preloaded in an aluminum pan and then inserted into the platinum basket.

DOI: 10.1021/acs.biomac.5b00977
Biomacromolecules XXXX, XXX, XXX−XXX

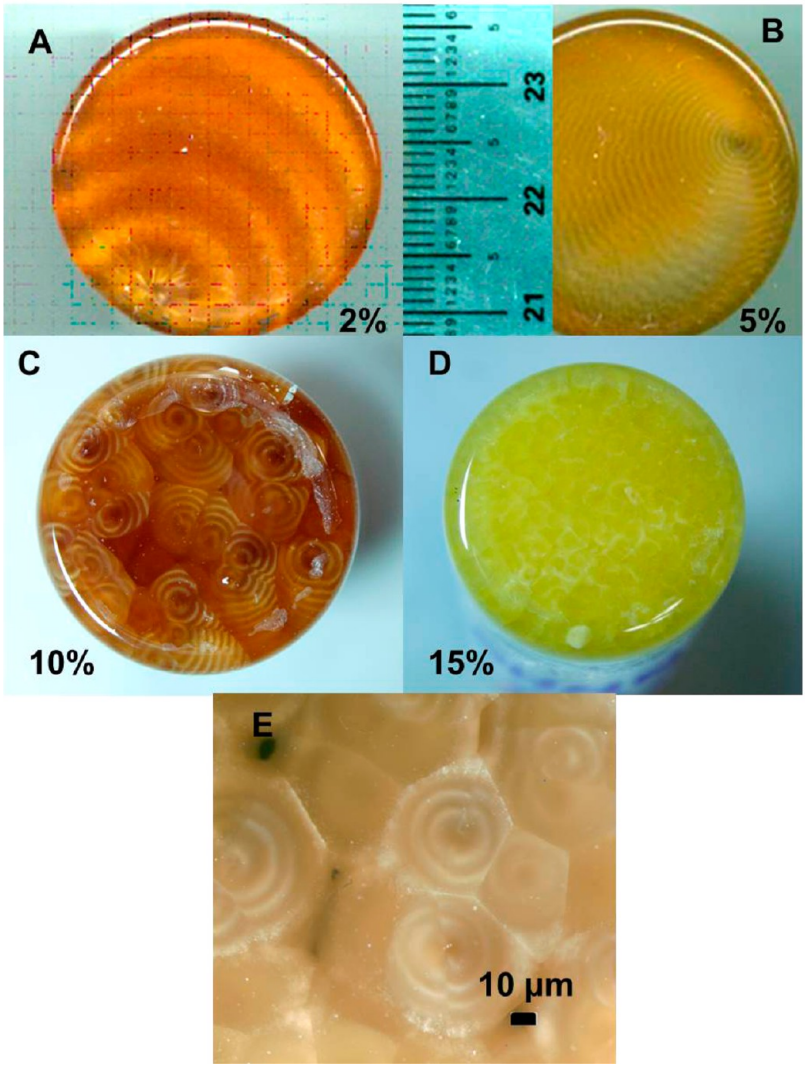

Figure 1. Concentric rings formed by (A) 2, (B) 5, (C) 10, and (D) 15% solutions of glu-6 in NMMO monohydrate; the unit of the scale bar in (B) is 1 mm. Pictures (A–D) were taken with a Canon EOS Digital Rebel XT (focal length 55 mm) camera. (E) Optical microscopy image in reflection mode representing spirals enclosed in polygonal shapes; the concentration of the glu-6-NMMO monohydrate solution is 10%. The bottom of each vial is 25 mm.

Small- and Wide-Angle X-ray Scattering, SAXS/WAXS. SAXS/WAXS measurements were recorded at Beamline 1–4 at the Stanford Synchrotron Radiation Laboratory, SSRL, Stanford, CA and at the Center for Advanced Microstructures and Devices, CAMD, Louisiana State University. The SAXS beamline at SSRL used a high-flux beam at 8.333 keV from a bending magnet within the 3 GeV storage ring. The beam was focused in the vertical plane by a platinum-coated mirror and focused in the horizontal plane by bending the Si [1 1 1] monochromating crystal. The detector was a MAR CCD array, with 2048 × 2048 pixels. The CAMD SAXS beamline uses a crystal monochromator tuned for 8 keV. The scattering pattern was recorded by using a Gabriel-style multiwire detector (Molecular Metronics, now Rikagu) having a 200 mm active diameter and a resolution of 200–500 μm fwhm in a 1024 × 1024 array. The CAMD storage ring operates at 1.3 GeV.

Rheology. A HAAKE Rheostress RS75 instrument provided with 4 cm stainless steel parallel plate geometry was used in oscillation mode. A frequency sequence program of 0.1–50 Hz and a heating rate of 2 °C·min^{-1}) was used to determine the rheological properties of polymer solutions, specifically, the G' and G'' moduli.

RESULTS AND DISCUSSION

Visual Observation and Microscopy. Upon unassisted cooling, D-glucaric acid-based polyamide solutions in NMMO·H_2O displayed patterns resembling spirals, as presented in Figure 1.

At low concentration, especially 5%, the self-organized spirals resemble rings formed annually in trees. While the sampling thickness and surface available for deposition were constant for all samples, the spiral/ring number and size varied as a function of concentration. For instance, in Figure 1A,B, a single nucleation event was observed, but the ring number increased while their pitch decreased for 5% when compared to 2% solution. Elevation in polymer concentration generated multiple nucleation points, as shown in Figure 1C,D (also see Figure S5, Supporting Information). The number of spirals and their associated rings increased, while the ring pitch decreased. Highly concentrated 70 and 80% solutions (Figure S6, Supporting Information) did not self-organize into spirals. The number of nucleation points that ultimately grew into concentric rings at higher concentrations can be correlated with the total amount of polymer in solution, which is expected to

DOI: 10.1021/acs.biomac.5b00977
Biomacromolecules XXXX, XXX, XXX–XXX

bring more impurities into the system (e.g., molecular defects). Figure S7 (Supporting Information) shows comparative images of nucleation at different times for different concentrations. The images also show that the spirals occur in both clockwise and counterclockwise disposition.

Most samples were prepared at the bottom of scintillation vials (25 mm diameter), and the thickness of the solutions was kept constant at 7 mm. Two extreme concentrations (2 and 80%) were prepared using vials with larger diameter (40 mm) to determine whether the surface available for growth is an important factor in the ringed spiral formation. The amount of solution was identical to that for the initial samples. Indeed, the ring diameter and its pitch increased over that seen in 2% solution (25 mm diameter), but the highest concentration failed again to show ring formation. While the effect of polymer molecular weight remains under investigation, 10% glu-6 in NMMO monohydrate solutions, prepared from different batches of glu-6, were casted on glass. All solutions self-organized in ringed spiral patterns (see Figure S5, Supporting Information). Optical microscopy brought to light another aspect. Figure 1E shows that each set of rings formed from solutions of the >10% polymer in NMMO monohydrate is enclosed in a polygonal shape, namely, pentagonal or hexagonal. These enclosures are most likely due to the growth of spirals into each other.

Solutions of D-galactaric acid-based polyamides in NMMO monohydrate did appear to self-organize, but no rings or spirals were observed. Their self-organized architecture resembled a butterfly appearance (Figure 4B). Upon changing the solvent to 1-butyl-3-methylimidazolium chloride, BMIMCl, solutions displayed patterns featuring wavy spiral orientation (Figure 2). The self-organization process took place over almost 2

Figure 2. Self-organized pattern of gal-6 in BMIMCl. The concentration of the solution is 10%, and the diameter of the vial is 25 mm.

weeks upon unassisted cooling, followed by aging at −15 °C. When 1-butyl-3-methylimidazolium acetate, BMIMAc, was used as solvent, ring/spiral formation was not observed.

In transmission microscopy between crossed polarizers, solutions of glu-6 in NMMO monohydrate exhibited optical anisotropy, as shown in Figure 3. The images show similar behavior as cellulosic solutions, known to develop liquid

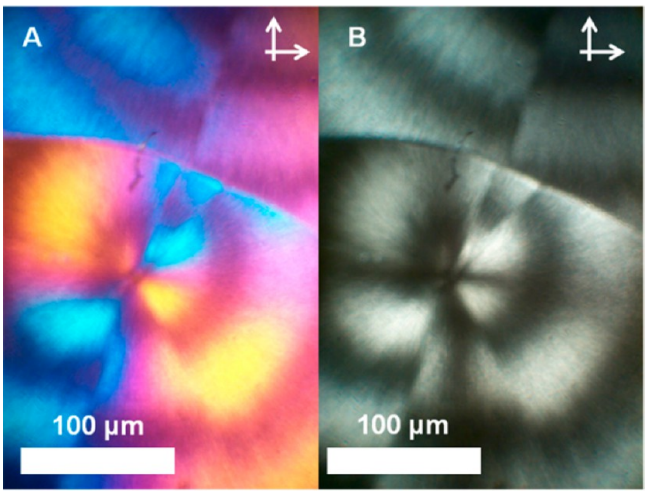

Figure 3. Polarized light micrographs of spirals formed in a 10% solution of glu-6 in NMMO monohydrate between crossed polarizers: (A) color plate and (B) no color plate.

crystalline order in NMMO·H_2O.[45] Additional polarized optical micrographs are available in Supporting Information, Figure S8.

Inspection with reflection microscopy (Figure 4) revealed new information about the spiral morphology. The nature of the surface available for growth appeared to impact the spatial disposition of the rings. Patterns grown on an untreated glass tended to grow flat on the surface, Figure 4A. Therefore, the solution mixture had high affinity for negatively charged glass. Polystyrene square cuvettes favored a mountain-like tilted orientation, Figure 4B.

The images displayed in Figure 4 suggest that the nature of the substrate upon which samples were cast induces a different appearance of the spirals. They do "stick" and grow flat on the untreated glass surface. On the other hand, the growth front seemed to be rejected by the polystyrene cuvette's wall, resulting in a mountain-like orientation (Figure 4B). Both sets of rings, lighter and darker, had a fibril-like appearance. NMMO monohydrate itself does not exhibit such organization (Figure 4D). The optical investigations point to self-organization taking place in the polymer solutions as a consequence of polymer−solvent interactions.

Solutions from glu-6 were compared to gal-6 in an attempt to assess the impact of sugar moiety stereochemistry on pattern formation. The gal-6 did not organize into a spiral disposition, as observed for glu-6 in NMMO monohydrate. Gal-6 solutions adopted a butterfly-like orientation, as shown in Figure 4C. Thus, the sugar molecular structure likely plays a role in pattern formation. First, the glucose backbone is asymmetric, while that of galactose is symmetric. Also, amide bonds are rigid by nature, and the flexibility of the chains comes from the freedom to rotate around C−C bonds. It can be hypothesized that symbiosis between glucose asymmetry, strong H-bonding with the solvent forces the chains to organize into a phase that requires the lowest energy possible.

The periodic structures of glu-6 were also investigated by Fourier Transform Infrared Microspectroscopy, micro-FTIR to identify whether new chemical species were present in the glu-6−NMMO mixtures after cooling. Spectra were collected from both dark and light rings of the spirals. Data are available in the Supporting Information, Figure S10. The results support the presence of strong H-bonding in the glu-6 solutions, and no evidence that spiral formation is a result of chemical reaction

DOI: 10.1021/acs.biomac.5b00977
Biomacromolecules XXXX, XXX, XXX−XXX

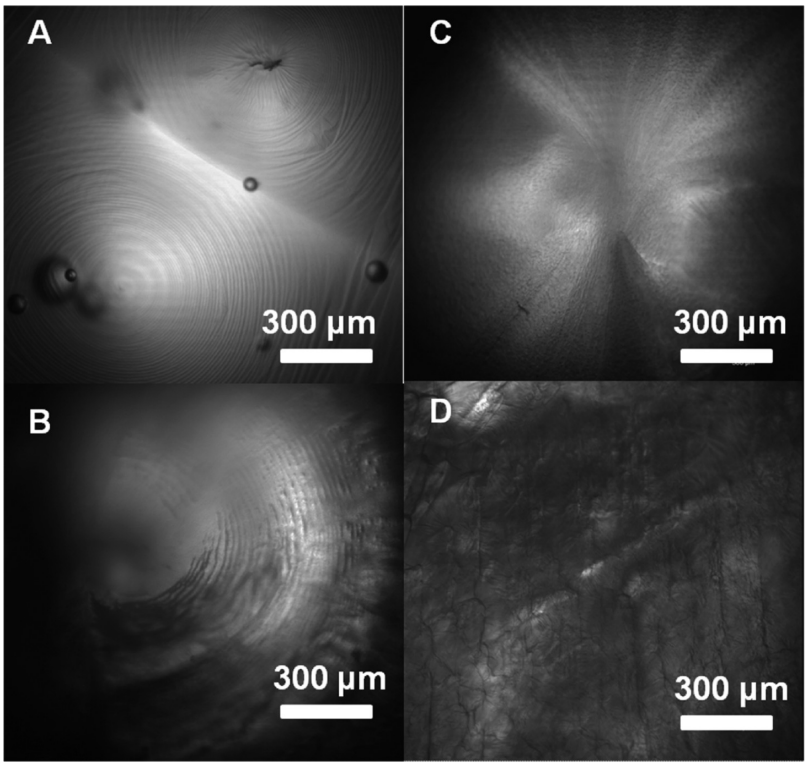

Figure 4. Reflection microscopy images of the 15% glu-6 solution in NMMO·H_2O between glass slides (A) and on a polystyrene surface (B); 10% gal-6 solution of NMMO·H_2O between glass slides (C) and the solvent, NMMO·H_2O on glass substrate (D).

was detected. Furthermore, the same concentration solutions were prepared from protected D-glucaric and D-galactaric-based polymers. Upon ambient cooling, they failed to organize into any kind of periodic pattern, nor were periodic structures observed for samples maintained at −15 °C for at least 2 weeks.

Additional tests were performed on a 10% Glu-6-NMMO·H_2O solution. Upon heating to ∼80 °C, it became an amber transparent fluid and the spirals disappeared. Then, the mixture was allowed to cool to room temperature by standing. The spirals nucleated and grew again, as depicted in Figure S7 (Supporting Information). The heating−cooling cycle was repeated four times; each time the spirals formed in the same manner, suggesting a reversible process. The same procedure was applied in the case of the polystyrene substrates. Altogether, these observations indicate that interactions between polymers carrying monosaccharide moieties with pendant hydroxyl groups and the solvent are the driving factor in spiral formation.

Thermal Behavior of Glu-6 Solutions in NMMO Monohydrate. Before analyzing the solutions, it was necessary to understand the thermal behavior of the solvent. Used for Lyocell fiber production or cellulose films from melt,[46−53] NMMO monohydrate is probably one of the most intriguing solvents aside from ionic liquids. Simple evaporation of water from a dilute aqueous NMMO solution results in a variety of hydrates where the number of hydration, *n*, spans from 0 to values greater than 2.5. Various studies have been carried out to understand the phase behavior of the NMMO hydrates.[47,54−56]

Melting temperatures have been reported for NMMO monohydrate at 72,[57] 75,[58] 75.6,[59] and 78 °C.[55] These discrepancies can be assigned to different instrumentation (calibration) and slight water content variation that impacts the DSC signal. The melting maximum found in this work was centered at 73.5 °C in heating mode, as shown in Figure 5. A previously reported crystallization event was also noted at much

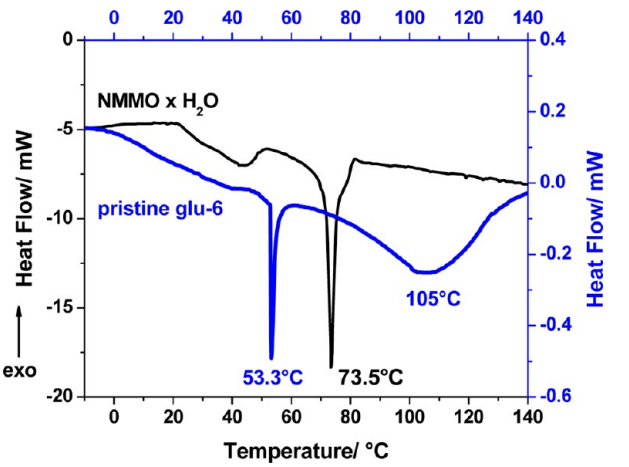

Figure 5. DSC traces on heating for NMMO monohydrate and pristine D-glucaric acid-based polyamide obtained in heating mode at a scan rate of 5 °C·min^{-1}.

lower temperature, 32.8 °C,[55] for NMMO monohydrate. Solutions of glu-6 in NMMO·H_2O showed sharp melting behavior at 53.3 °C followed by a broad endothermic event at 105 °C.

Dilute solutions of glu-6 behaved slightly different than concentrated ones. The thermogram for a 2% glu-6-NMMO monohydrate mixture in the first heating mode (Figure 6A) was identical to that of the simple solvent, while 5 and 10% shifted to a slightly smaller value. Upon cooling, the first crystallization event (Figure 6B) shifted to higher values in the case of the

DOI: 10.1021/acs.biomac.5b00977
Biomacromolecules XXXX, XXX, XXX−XXX

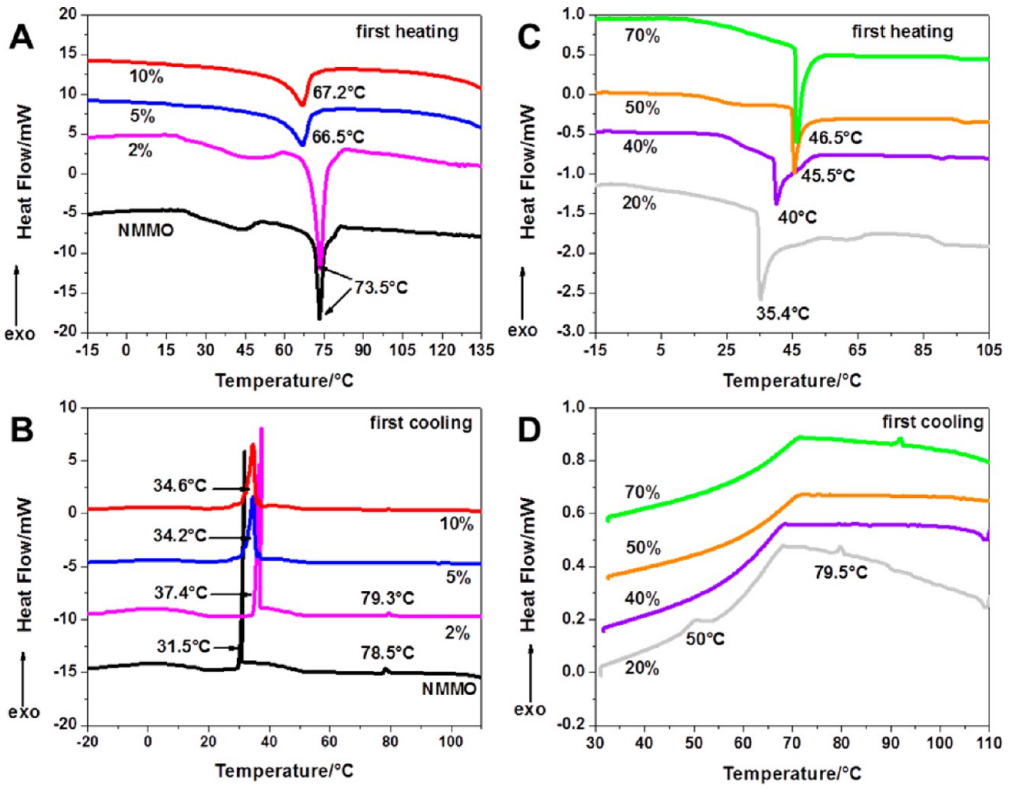

Figure 6. DSC traces of dilute solutions of glu-6 in NMMO monohydrate recorded on (A) first heating and (B) first cooling, and concentrated solutions recorded on (C) first cooling and (D) first heating modes. Scan rate was 5 °C·min^{-1}.

most dilute solution (2%). Solutions of 5 and 10% polymer content tended to align close to the value recorded for NMMO monohydrate, 31.5 °C. The second crystallization of the solvent (78.5 °C) was observed only in the 2% solution (79.3 °C). The first depressed melting point recorded for solvent at 73.5 °C occurred at the same value in the 2% polyamide solution, but was shifted to lower temperature for 5 (66.5 °C) and 10% (67.2 °C).

Concentrated solutions exhibited depressed crystalline melting temperatures according to the polymer amount present in the system. On the first heating mode shown in Figure 6C, the temperature range of these endothermic events shifted from 35.4 °C (20%) to 46.5 °C (50 and 70%). The low crystalline peak noticed in the first cooling mode for dilute solutions was visible for 20% (79.5 °C), but not for medium-concentrated solutions (Figure 6D). A possible small reminder of solvent crystallization was found at 90 °C for a 70% glu-6 solution. The endothermic peak centered at 50 °C on cooling (Figure 6D, 20%) can be assigned to the phase transition from the simple liquid (isotropic) to a liquid crystalline phase (anisotropic). The second heating and cooling modes appear in Figure S2, Supporting Information.

As mentioned earlier, NMMO can form a variety of hydrates. This investigation used the monohydrate form, which is the solvent for spinning Lyocell rayon fibers.[46,51,53,54] Nonetheless, during sample preparation, even though a nitrogen atmosphere was ensured at all times, small traces of water were absorbed into the mixtures resulting in a slight increase in hydration number, n (see Supporting Information, Karl Fischer titration). Therefore, the applications of these sugar-based polyamide mixtures directed toward processing (e.g., fiber spinning) should take into account the fact that, at the same composition and temperature, the phase of the spinning solution might in fact be different from that of processed fiber.

Small/Wide Angle X-ray Scattering. Small- and wide-angle X-ray scattering measurements were conducted to learn whether any ordered features were present in the solution or even in the solvent itself, which might contain structures to accommodate water. All scattering patterns were circular, without any indication of alignment or ordering during the loading of the samples into X-ray capillaries. The solution exhibited a well-defined ring at a d-spacing of 15.5 Å. A number of other peaks were observed (Figure S13, Supporting Information). Complete indexing of the crystal structure was not possible, but for the sake of future reference, the observed d-spacing values are listed in the Supporting Information, Table S4. There does appear to be a cubic structure with primary d-spacing of 6.2 Å, but other peaks could not be assigned. These peaks can originate from various coexisting forms of crystalline solvent and solvated NMMO-glu-6 crystals. The content in the NMMO monohydrate crystalline phases depends on hydration number; multiple forms were observed for $n \geq 1$.[60] The multiplicity of peaks leaves open the future possibility that nanoscale structure can be correlated with the visible patterns by using microbeam "imaging" SAXS/WAXS methods.[61]

Rheology. Sugar-based polyamides can be used to spin fibers, to cast films, and in green packaging. The feasibility of processing these polyamides was investigated by rheology because the final product quality depends on the mechanical properties of the polymeric constituent. The two parameters, dynamic viscosity, η (the ratio between the viscous modulus, G'', and frequency) and tan δ (the ratio of G'' and elastic modulus, G') displayed in Figure 7 show the rheological behavior of 80% glu-6 solution in NMMO monohydrate.

DOI: 10.1021/acs.biomac.5b00977
Biomacromolecules XXXX, XXX, XXX−XXX

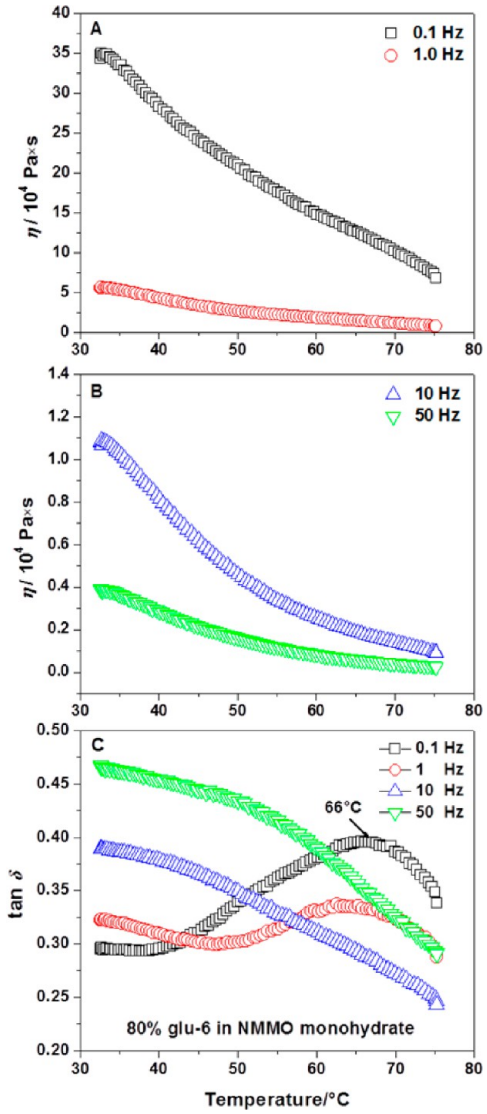

Figure 7. Dynamic viscosity, η (A, B) and tan δ (C) as a function of temperature and frequency of the 80% glu-6 solution in NMMO monohydrate.

The dynamic viscosity is not very far removed from Arrhenius behavior at any temperature, as shown in Figure 8, although some curvature is evident at 50 Hz. The activation energy values appear in Table S5 and Figure S14, Supporting Information.

At the two lowest frequencies, there is a modest "wrinkle" at $T \cong 50$ °C ($1/T = 0.0031$ K^{-1}). The tan δ value, Figure 7C, bumps up at these frequencies at ~66 °C, suggesting a new loss mechanism, due to melting of some indeterminate structure. Confirmation of the structural implications by rheo-optical or rheo-scattering methods is beyond the scope of this study.

H-Bonding as an Essential Factor in Spiral Formation. The process behind the formation of ringed spirals upon ambient cooling solutions of glu-6 and gal-6 in NMMO monohydrate can be explained by the presence of solvent−solvent and solvent−polymer H-bonding. To some extent, the behavior of glu-6 in NMMO monohydrate should be similar to that of cellulose in the same solvent.[62−66] These two polymers share the same unit: glucose. Because the crystallization of the solvent appears to play an important role in the formation of

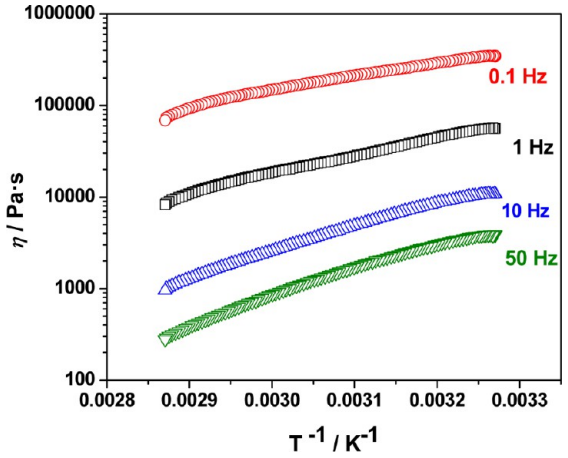

Figure 8. Arrhenius representation of dynamic viscosity vs inverse temperature at different frequencies.

ring morphologies (see Figures 5, 6, and 7), it was essential to first understand the crystal formation,[67] the elucidation of the crystal structure,[68] and the conformer distribution[69] of NMMO monohydrate. Computational studies based on $J-J$ coupling constants and associated energies revealed two chair conformations with axial N−O and equatorial N−O, two boat conformers, and one twist conformation.[69] Due to the energy gap between all possible conformers, below decomposition temperature, only the chair conformers should be present in the solution. Interactions of N−O, whose dipole moment was calculated to be 4.4 D,[70] with polar solvents promoted the stabilization of the chair through the equatorial oxygen.

The two polymers capable of self-organization into spirals and butterfly-like patterns are not water-soluble due to the strong H-bonding between free hydroxyl groups attached to the sugar backbone units. Consequently, the polyamides are difficult to characterize in aqueous solutions. On the contrary, in the self-organization process, water is a third party, playing an important role. For example, in nature, water has the potential to influence the radial growth in trees.[71−73] Furthermore, rock concretionary geometries resembling asymmetrical mineralization and banded precipitation patterns (Liesegang bands) were closely related with the seasonal precipitation levels.[74] Polymers do not dissolve due to the strong intramolecular H-bonding, but their "solid" form nevertheless lacks permanence: water can slowly infiltrate and alter its structure. In the case of glu-6-NMMO solutions, the disruption of the native H-bonding within each molecule and between NMMO and water must evolve concurrently with the formation of the new H-bond network, which favors self-organization of the system until the equilibrium is reached. This sequence of events can also be viewed as a process able to promote the formation of two nascent phases, one richer in the crystallizable component (NMMO-glu-6) and the other containing relatively more amorphous polymer. The existence of these phases can also offer the interface for heterogeneous nucleation[75] only if the overall system free energy is much lower than that associated with homogeneous nucleation. Moreover, the free energy barrier for nucleation is significantly reduced when impurities are present. Hence, the heterogeneous process can take the leading role over the homogeneous one. After mixing, the preparation is comprised of three phases: NMMO-glu-6 complex, nonsolvated amorphous polymer, and free solvent. Three regimes can be distinguished in self-

DOI: 10.1021/acs.biomac.5b00977
Biomacromolecules XXXX, XXX, XXX−XXX

organization of these polyamide solutions. First, below a critical polymer concentration value, the formation of periodic patterns was not observed. The amount of polymer is insignificant and does not affect solvent nucleation into regular morphologies. Solutions of 1% glu-6 crystallized into patterns similar to those of free solvent (branched structures). Second, the domain of self-organization was noticed to span the concentration range between 2 and 40%. Third, above the critical concentration (40%), concentric rings did not form. The high amount of polymer brings with it a high number of impurities, such as dust, molecular defects, and polydispersity. Solutions might nucleate heterogeneously, but the multitude of incipient nuclei cannot have enough energy to grow into an organized structure.

Water coexists as H-bonded to NMMO and glu-6 and, most likely, also in free form, expelled from the H-bonding interchange. The water content can be evaluated from the thermogravimetric analysis (Figure S15, Supporting Information). The amount of energy necessary to break the H-bonds can be considered up to 250 °C. Both pristine glu-6 and solvent displayed a broad peak close to 250 °C, suggesting strong H-bonding interactions. In the solution state, the peak in derivative of mass loss, DTG, curve shifts to the lower values of temperature. An 80% solution has a sharp peak situated between 175 and 200 °C.

Spiral Characterization: A Quantitative Approach. The variation in thickness of the pattern rings as a function of concentration was computed from the images of the spirals, as shown in Figure S16 (Supporting Information). Figure 9A reflects the thickness of the second ring calculated for the concentration range 5−20%. The thickness of the ring decreased with increased concentration. The fit of the data shows a first-order exponential decay trend. The thickness of the rings decreased while their number increased with the increase in concentration, Figure 9B.

The cooling method played a role in determining the size of the self-organized patterns. Samples of the same concentration cooled under ambient conditions at room temperature showed larger, more confined rings when compared with those subjected to cooling by refrigeration. The formation of the rings from D-galactaric acid-based polyamides in BMIMCl seems to follow the same quantitative trend as their glucaric acid-based counterparts in NMMO monohydrate.

Pathways to the Spiral Formation. Because glu-6 and gal-6 are polycondensates between diacid and diamine units connected through amide bonds, which are much more rigid than C−O−C links between glucosyl units from cellulose, two pathways are proposed for the self-organization mechanism using glu-6 and NMMO monohydrate as an example. The first route involves solvent-mediated inter- and intramolecular H-bonding (Scheme 1a,b). The second, and somewhat less-likely, pathway is mediated by the amide bonds (Scheme S1, Supporting Information).

NMMO possesses a very strongly polar N−O bond that interacts with two molecules of water linked through H-bonds.[60] Once the ternary component glu-6, is added in the biphasic solvent, water molecules begin to "sense" the free pairs of electrons from amidic O and N. This interaction might initiate the delocalization of the amidic nitrogen's free electrons in the amide-mediated pathway. In this way, the amidic O becomes more electron-rich. Water interaction with both NMMO and the polymer's amidic group can lessen the influence from the NMMO's N−O polar group. Consequently,

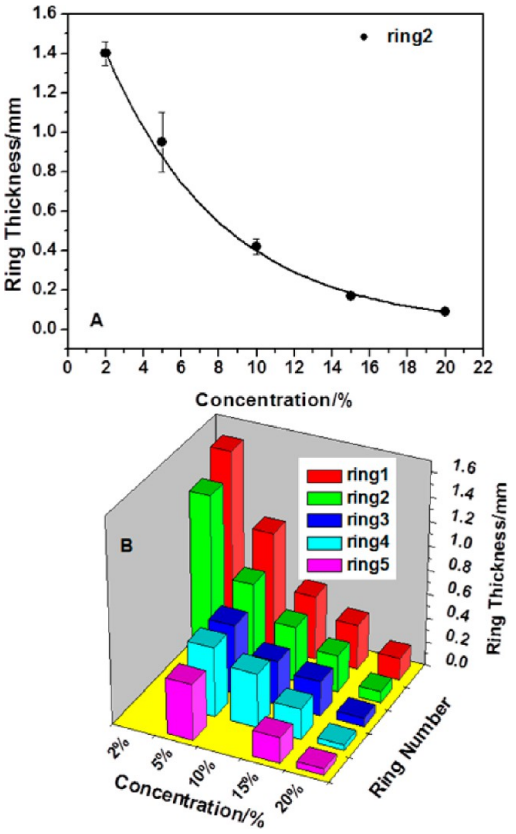

Figure 9. Variation of ring thickness as a function of concentration (A, the error bar for the last two data points are smaller than the point) and evolution of ring number and thickness as a function of concentration (B).

the solvent is free to compete and directly interact with the amide group, expelling the intra-H-bonded water. The impact of this interaction on polymer units would result in polymer chain stiffening. Water can be then H-bonded with either OH groups from the glu-6 backbone or with the excess bulk solvent in the case of dilute solutions.

Turning now to discuss the first pathway, intermolecular H-bonding, Scheme 1a, is based on the interactions between the N−O polar group and the secondary hydroxyl groups from two adjacent glu-6 backbone glucose units. It was shown that the less polar chair conformation of NMMO monohydrate with axial oxygen was favored by the presence of a sugar such as cellobiose pendant to glucose bridged in the $\beta(1-4)$ position.[69] Because the glucuronic acid had a small effect on the NMMO conformer equilibrium, it was believed that the interaction between glucose and NMMO occurred mainly with C6 hydroxyls. Scheme 1a shows H-bonding formed between OH (**3**) from two consecutive glucosyl residues and NMMO monohydrate. Steric hindrance hampers the interaction of NMMO's N−O site with hydroxyls belonging to consecutive carbons from the same glucose residue. As a result of this interaction, water may begin to be expelled from immediate proximity of the N−O group. After H-bonding rearrangement, water can be involved in H-bonded networks with the remaining free hydroxyls of glucose. The linkages formed between two different OH bonds belonging to different units cause a strong stiffening of the chains. The rotation along the C−C bond is restricted due to these H-bridges. Finally, the possibility that H-bonds can also be initiated between OH (**2**)

DOI: 10.1021/acs.biomac.5b00977
Biomacromolecules XXXX, XXX, XXX−XXX

Scheme 1. Idealized Pathways of Interaction between the N−O Polar Group of the Solvent and Glucose Secondary Hydroxyl Groups

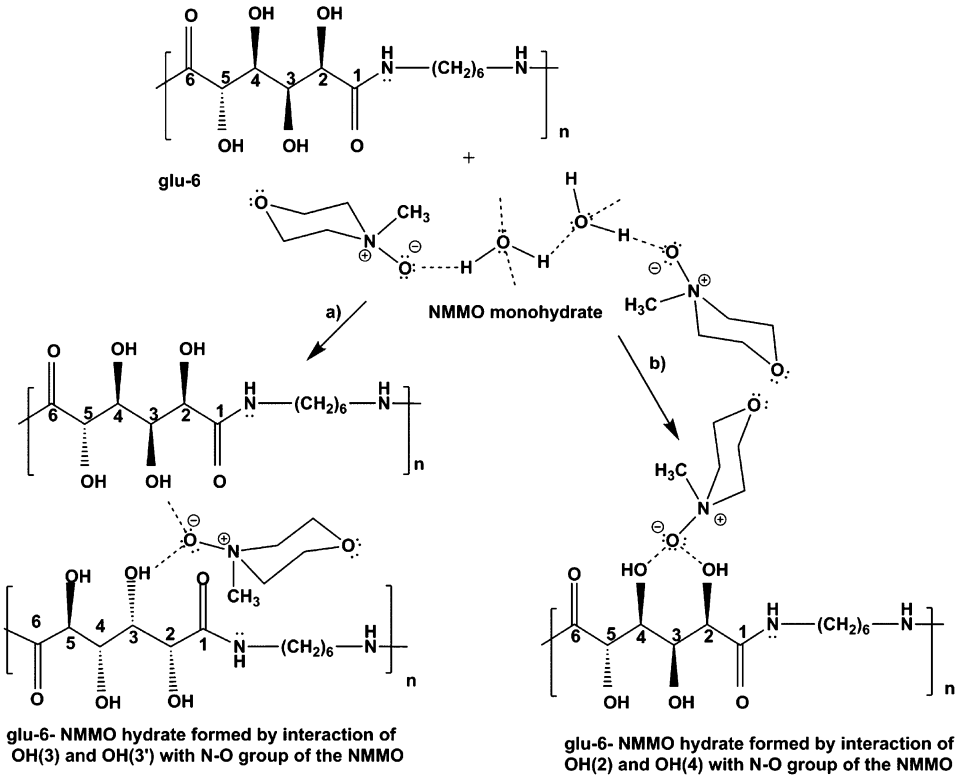

and OH (**4**) from the same unit should be taken into account (Scheme 1b). Similar hydrogen-bonding between sugar units was also considered the determinant factor in the formation of spherulites from melts of carbohydrate-based polyamides.[76]

In order to test the role of the free hydroxyl groups on system self-assembly, control experiments have been performed on ketal-protected polyamides.[40] They did not show any tendency to self-organize into patterns such as rings or any other morphology.

CONCLUSIONS

Solutions of the polyamide formed by D-glucaric acid and 1,6-hexamethylene diamine in NMMO monohydrate were found to self-organize in patterns resembling concentric rings upon unassisted cooling to ambient temperature. The size of the spirals and rings depended strongly on concentration, cooling methodology and temperature. The number of spirals and their rings increased with concentration while the ring pitch decreased. Polyamides from D-galactaric acid self-organized into different shapes. In NMMO monohydrate they resembled a butterfly like morphology. Consequently, the structure and symmetry of the two sugar units coupled to a strong H-bonding with the solvent impacted the morphology of the cooled solutions. D-Galactaric acid-based polyamide displayed ring formation when its solution in BMIMCl was cooled at −15 °C over a period of almost 2 weeks. No such fringes were noticed when an alternate ionic liquid, BMIMAc, was used.

Placed between crossed polarizers, polymer solutions in NMMO monohydrate showed birefringence, similar to reports on cellulose. The formation of these patterns can be explained by a rearrangement of the polymer intramolecular H-bonding to permit the formation of H-bonds with NMMO monohydrate. This hypothesis was tested by using corresponding polymers from ketal-protected D-galactaric acid. Their solutions in NMMO monohydrate failed to organize into ring patterns. Two pathways are plausible, but experimental data points mostly to the formation of new H-bond networks between solvent's N−O polar group and secondary hydroxyls, either OH (**3**) or OH (**2**)/OH (**4**) of two adjacent glucosyl units. The content of water in these solutions and a supplemental proof on H-bonding reorganization was provided by thermogravimetric and micro-IR analysis. Thermal behavior of the polyamides and their solutions in NMMO monohydrate is tightly related to the polymer concentration.

SAXS/WAXS measurements revealed the existence of a polycrystalline glu-6-NMMO monohydrate system. Above the anisotropic−isotropic transition (∼50 °C), the dynamic viscosity depends more weakly on temperature than in anisotropic region. The intense increase in storage modulus in the anisotropic zone is probably due to polymer relative high polydispersity. This trend causes transition "smearing" in the dynamic viscosity as a function of temperature behavior. The rheology of the sugar-based polyamide solutions in NMMO monohydrate confirmed the optimum mechanical characteristics necessary to process these solutions into fibers by spinning and films by solution casting. The self-organized systems can also serve as good models for understanding and simulating biomimetic materials and other more complex and spectacular phenomena occurring either in nature or in the laboratory.

ASSOCIATED CONTENT

Supporting Information

Experimental details, POM, DSC, TGA, and micro-FTIR supplementary data, SAXS/WAXS data analysis details, and proposed amide activation pathway for spiral formation. The

DOI: 10.1021/acs.biomac.5b00977
Biomacromolecules XXXX, XXX, XXX−XXX

Supporting Information is available free of charge on the ACS Publications website at DOI: 10.1021/acs.biomac.5b00977.

(PDF)

AUTHOR INFORMATION

Corresponding Authors

*E-mail: cornelia.rosu@mse.gatech.edu.

*E-mail: inegule@lsu.edu.

Notes

The authors declare no competing financial interest.

ACKNOWLEDGMENTS

This work was supported partially by (I.I.N.) the USDA multistate Hatch Program S-1041 LSU (Ag. Center; P.S.R.), National Science Foundation Awards under Grant 1306262 (DMR) and through the generosity of the Hightower Family (C.R.). The authors are grateful to Cindy Henk and Dr. Mathew Brown (Socolofski Microscopy Center, Louisiana State University) for technical support in microscopic measurements, Mihaela Cucu-Wheeler (now working at Johnson & Johnson, Rochester, NY) for recording 2 and 5% glu-6-NMMO monohydrate solution optical images seen in the main text. The help of Andrew Weber (CAMD, Louisiana State University) with WAXS measurements and Dr. Orhan Kizilkaya with IR investigations is also acknowledged. C.R. is deeply thankful to Professors Seth Fraden (Martin A. Fisher School of Physics, Brandeis University, Waltham, MA), John Pojman and Evgueni Nesterov (Chemistry Department, Louisiana State University, Baton Rouge, LA), Elsa Reichmanis (School of Chemical and Biomolecular Engineering, School of Chemistry and Biochemistry, School of Materials Science and Engineering, Georgia Institute of Technology, Atlanta, Georgia), and Professor Dilip Kondepudi (Chemistry Department, Wake-Forest University, Winston-Salem, NC), as well as to Professor David Bucknall (School of Materials Science and Engineering, Georgia Institute of Technology, Atlanta, GA) for helpful suggestions.

REFERENCES

(1) Hosier, I. L.; Bassett, D. C.; Vaughan, A. S. Spherulitic Growth and Cellulation in Dilute Blends of Monodisperse Long n-Alkanes. *Macromolecules* **2000**, *33* (23), 8781−8790.

(2) Hutter, J. L.; Bechhoefer, J. Morphology transitions in diffusion- and kinetics-limited solidification of a liquid crystal. *Phys. Rev. E: Stat. Phys., Plasmas, Fluids, Relat. Interdiscip. Top.* **1999**, *59* (4), 4342−4352.

(3) Hutter, J. L.; Bechhoefer, J. Banded spherulitic growth in a liquid crystal. *J. Cryst. Growth* **2000**, *217* (3), 332−343.

(4) Lotz, B.; Wittmann, J. C. Structural relationships in blends of isotactic polypropylene and polymers with aliphatic sequences. *J. Polym. Sci., Part B: Polym. Phys.* **1986**, *24* (7), 1559−75.

(5) Norton, D. R.; Keller, A. The spherulitic and lamellar morphology of melt-crystallized isotactic polypropylene. *Polymer* **1985**, *26* (5), 704−16.

(6) Ryschenkow, G.; Faivre, G. Bulk crystallization of liquid selenium. Primary nucleation, growth kinetics and modes of crystallization. *J. Cryst. Growth* **1988**, *87* (2−3), 221−35.

(7) Bisault, J.; Ryschenkow, G.; Faivre, G. Spherulitic branching in the crystallization of liquid selenium. *J. Cryst. Growth* **1991**, *110* (4), 889−909.

(8) Morse, H. W.; Warren, C. H.; Donnay, J. D. H. Artificial spherulites and related aggregates. *Am. J. Sci.* **1932**, *23*, 421−439.

(9) Magill, J. H.; Plazek, D. J. Physical properties of aromatic hydrocarbons 0.2. Solidification behavior of 1,3,5-tri-alpha-naphthyl-benzene. *J. Chem. Phys.* **1967**, *46* (10), 3757−3769.

(10) Magill, J. H. Spherulites: a personal perspective. *J. Mater. Sci.* **2001**, *36* (13), 3143−3164.

(11) Sperling, L. H. *Introduction to Physical Polymer Science*; Wiley: New York, 1992; Chapter 6.

(12) Phillips, P. J. *Handbook of Crystal Growth*; Elsevier: Amsterdam, 1993; Vol. 2, Chapter 18.

(13) Padden, F. J., Jr.; Keith, H. D. Crystalline morphology of synthetic polypepfides. *J. Appl. Phys.* **1965**, *36* (10), 2987−95.

(14) Granasy, L.; Pusztai, T.; Tegze, G.; Warren, J. A.; Douglas, J. F. Growth and form of spherulites. *Phys. Rev. E: Stat., Nonlinear, Soft Matter Phys.* **2005**, *72* (1), 011605.

(15) Shtukenberg, A. G.; Punin, Y. O.; Gunn, E.; Kahr, B. Spherulites. *Chem. Rev.* **2012**, *112* (3), 1805−1838.

(16) Ramanathan, M.; Darling, S. B. Mesoscale morphologies in polymer thin films. *Prog. Polym. Sci.* **2011**, *36* (6), 793−812.

(17) Keith, H. D.; Padden, F. J. Ringed spherulites in polyethylene. *J. Polym. Sci.* **1958**, *31* (123), 415−421.

(18) Schuur, G. Mechanism of the crystallization of high polymers. *J. Polym. Sci.* **1953**, *11* (5), 385−398.

(19) Keith, H. D.; Padden, F. J. A phenomenological theory of spherulitic crystallization. *J. Appl. Phys.* **1963**, *34* (8), 2409−2421.

(20) Liesegang, R. E. *Naturwiss. Wochencshr.* **1896**, *11*, 353−362.

(21) Turing, A. M. The chemical basis of morphogenesis. *Philos. Trans. R. Soc., B* **1952**, *237* (641), 37−72.

(22) Mikhailov, A. S.; Krinsky, V. I. Rotating spiral waves in excitable media - the analytical results. *Phys. D* **1983**, *9* (3), 346−371.

(23) Zykov, V. S. Cycloidal circulation of spiral waves in excitable medium. *Biofizika* **1986**, *31* (5), 862−865.

(24) Biton, Y.; Rabinovitch, A.; Braunstein, D.; Friedman, M.; Aviram, I. Three-dimensional recurring patterns in excitable media. *Phys. Lett. A* **2011**, *375* (24), 2333−2337.

(25) Kupitz, D.; Alonso, S.; Bar, M.; Hauser, M. J. B. Surfactant-induced gradients in the three-dimensional Belousov-Zhabotinsky reaction. *Phys. Rev. E: Stat., Nonlinear, Soft Matter Phys.* **2011**, *84* (5), 056210.

(26) Manz, B.; Masere, J.; Pojman, J. A.; Volke, F. Magnetic resonance imaging of spiral patterns in crosslinked polymer gels produced via frontal polymerization. *J. Polym. Sci., Part A: Polym. Chem.* **2001**, *39* (7), 1075−1080.

(27) Pojman, J. A.; Masere, J.; Petretto, E.; Rustici, M.; Huh, D. S.; Kim, M. S.; Volpert, V. The effect of reactor geometry on frontal polymerization spin modes. *Chaos* **2002**, *12* (1), 56−65.

(28) Ostwald, W. Studien uber die Bildung und Umwandlung fester Korper. *Z. Phys. Chem.* **1897**, *22*, 289−300.

(29) Snyder, V. A.; Alkemper, J.; Voorhees, P. W. The development of spatial correlations during Ostwald ripening: A test of theory. *Acta Mater.* **2000**, *48* (10), 2689−2701.

(30) Wang, Y.; Chan, C. M.; Li, L.; Ng, K. M. Concentric-ringed structures in polymer thin films. *Langmuir* **2006**, *22* (17), 7384−7390.

(31) Nagarajan, V.; Zhang, K.; Misra, M.; Mohanty, A. K. Overcoming the Fundamental Challenges in Improving the Impact Strength and Crystallinity of PLA Biocomposites: Influence of Nucleating Agent and Mold Temperature. *ACS Appl. Mater. Interfaces* **2015**, *7* (21), 11203−11214.

(32) Ni'mah, H.; Woo, E. M. Effects of Glycine-Based Ionic Liquid on Spherulite Morphology of Poly(L-lactide). *Macromol. Chem. Phys.* **2015**, *216* (12), 1291−1301.

(33) Liu, L. J.; Li, S. M.; Garreau, H.; Vert, M. Selective enzymatic degradations of poly(L-lactide) and poly(epsilon-caprolactone) blend films. *Biomacromolecules* **2000**, *1* (3), 350−359.

(34) Abe, H.; Kikkawa, Y.; Inoue, Y.; Doi, Y. Morphological and kinetic analyses of regime transition for poly[(S)-lactide] crystal growth. *Biomacromolecules* **2001**, *2* (3), 1007−1014.

(35) Pan, P.; Liang, Z.; Zhu, B.; Dong, T.; Inoue, Y. Blending Effects on Polymorphic Crystallization of Poly(L-lactide). *Macromolecules* **2009**, *42* (9), 3374−3380.

(36) Teramoto, Y.; Nishio, Y. Biodegradable cellulose diacetate-graft-poly(L-lactide)s: Thermal treatment effect on the development of supramolecular structures. *Biomacromolecules* **2004**, *5* (2), 397−406.

DOI: 10.1021/acs.biomac.5b00977
Biomacromolecules XXXX, XXX, XXX−XXX

(37) Lee, L.-T.; Woo, E. M.; Hsieh, Y.-T. Macro- and micro-lamellar assembly and mechanisms for unusual large-pitch banding in poly(l-lactic acid). *Polymer* **2012**, *53* (23), 5313−5319.
(38) Dube, M.; Deslandes, Y.; Marchessault, R. H. Spherulitic precipitation of cellulose from amine-oxide solutions. *J. Polym. Sci., Polym. Lett. Ed.* **1984**, *22* (3), 163−171.
(39) Ding, M.; Yu, J.; He, J.; Zhang, J. An unusual spherulite morphology induced by nano-fillers from a concentrated cellulose/ionic liquid solution. *RSC Adv.* **2015**, *5* (55), 44648−44651.
(40) Rosu, C.; Negulescu, II; Cueto, R.; Laine, R.; Daly, W. H. Synthesis and Characterization of Complex Mixtures Consisting of Cyclic and Linear Polyamides from Ethyl Bis-Ketal Galactarates. *J. Macromol. Sci., Part A: Pure Appl.Chem.* **2013**, *50* (9), 940−952.
(41) Kiely, D. E.; Chen, L.; Lin, T. H. Hydroxylated nylons based on unprotected esterified D-glucaric acid by simple condensation-reactions. *J. Am. Chem. Soc.* **1994**, *116* (2), 571−578.
(42) Prompers, G.; Keul, H.; Hocker, H. Polyurethanes with pendant hydroxy groups: polycondensation of 1,6-bis-O-phenoxycarbonyl-2,3:4,5-di-O-isopropylidenegalactitol and 1,6-di-O-phenoxycarbonylgalactitol with diamines. *Green Chem.* **2006**, *8* (5), 467−478.
(43) Rosu, C. *Recent Advances in Glylon Science*. Thesis, Louisiana State University, Baton Rouge, LA, May, 2010.
(44) Dyson, P. J.; Grossel, M. C.; Srinivasan, N.; Vine, T.; Welton, T.; Williams, D. J.; White, A. J. P.; Zigras, T. Organometallic synthesis in ambient temperature chloroaluminate(III) ionic liquids. Ligand exchange reactions of ferrocene. *J. Chem. Soc., Dalton Trans.* **1997**, *19*, 3465−3469.
(45) Laszkiewicz, B. Liquid crystal phenomena in cellulose-NMMO-H2O system. *Mol. Cryst. Liq. Cryst. Sci. Technol., Sect. A* **2000**, *353*, 127−131.
(46) Graenacher, C.; Sallman, R. Cellulose solution and process of making some. U.S. Patent 2,179,181, April 1, 1937.
(47) Chanzy, H.; Peguy, A.; Chaunis, S.; Monzie, P. Oriented cellulose films and fibers from a mesophase system. *J. Polym. Sci., Polym. Phys. Ed.* **1980**, *18* (5), 1137−1144.
(48) Johnson, D. L. Compounds dissolved in cyclic amines oxides. U.S. Patent 3,447,939, Jun. 3, 1969.
(49) Johnson, D. L. Method for preparing polymers from a mixture of cyclic amine oxides and polymers. U.S. Patent 3,508,941, April 28, 1970.
(50) McCorsley, C. C.; Varga, J. K. Process for making a precursor of a solution of cellulose. U.S. Patent 4,142,913, Mar. 6, 1979.
(51) Franks, N. E.; Varga, S. K. Process for making precipitated cellulose. U.S. Patent 4,145,532, Mar. 20, 1979.
(52) Franks, N. E.; Varga, J. K. Process for making a shapeable cellulose and shaped cellulose products. U.S. Patent 4,196,282, April 1, 1980.
(53) McCorsley, C. C. Process for shaped cellulose article prepared from a solution containing cellulose dissolved in a tertiary amine N-oxide solvent. U.S. Patent 4,246,221, Jan. 20, 1981.
(54) Chanzy, H.; Paillet, M.; Hagege, R. Spinning of cellulose from n-methyl morpholine N-oxide in the presence of additives. *Polymer* **1990**, *31* (3), 400−405.
(55) Kim, D. B.; Lee, W. S.; Jo, S. M.; Lee, Y. M.; Kim, B. C. Effect of thermal history on the phase behavior of N-methyl morpholine N-oxide hydrates and their solutions of cellulose. *Polym. J.* **2001**, *33* (2), 139−146.
(56) Loubinoux, D.; Chaunis, S. An experimental approach to spinning new cellulose fibers with n-methylmorpholine-oxide as a solvent. *Text. Res. J.* **1987**, *57* (2), 61−65.
(57) Iovleva, M. M.; Smirnova, V. N.; Belousov, Y. Y.; Papkov, S. P. Evaluation of interactions of N-methylmorpholine-N-oxide hydrates with cellulose. *Polym. Sci. U.S.S.R.* **1986**, *28* (4), 749−752.
(58) Chanzy, H.; Nawrot, S.; Peguy, A.; Smith, P.; Chevalier, J. Phase-behavior of the quasi-ternary system N-methylmorpholine-N-oxide, water, and cellulose. *J. Polym. Sci., Polym. Phys. Ed.* **1982**, *20* (10), 1909−1924.
(59) Navard, P.; Haudin, J. M. Thermal study of N-methylmorpholine N-oxide and its complexing with water. *J. Therm. Anal.* **1981**, *22* (1), 107−118.
(60) Kim, D. B.; Jo, S. M.; Lee, W. S.; Pak, J. J. Physical agglomeration behavior in preparation of cellulose-N-methyl morpholine N-oxide hydrate solutions by simple mixing. *J. Appl. Polym. Sci.* **2004**, *93* (4), 1687−1697.
(61) Hayashida, K.; Kawashima, W.; Takano, A.; Shinohara, Y.; Amemiya, Y.; Nozue, Y.; Matsushita, Y. Archimedean tiling patterns of ABC star-shaped terpolymers studied by microbeam small-angle X-ray scattering. *Macromolecules* **2006**, *39* (14), 4869−4872.
(62) Gagnaire, D.; Mancier, D.; Vincendon, M. Cellulose organic solutions - nuclear magnetic-resonance investigation. *J. Polym. Sci., Polym. Chem. Ed.* **1980**, *18* (1), 13−25.
(63) Wagenknecht, W.; Loth, F. Dissolution of cellulose in mixtures of N-methylmorpholine-N-oxide, water and aliphatic amines. *Papier* **1998**, *52* (11), 643−647.
(64) Berger, W.; Keck, M.; Van Sang, D.; Philipp, B. UV-spectroscopic study on the interaction of cellulose and corresponding model substances with N-methyl-morpholin-N-oxid. *Z. Phys. Chem.* **1985**, *266* (3), 436−440.
(65) Fink, H. P.; Weigel, P.; Purz, H. J.; Ganster, J. Structure formation of regenerated cellulose materials from NMMO-solutions. *Prog. Polym. Sci.* **2001**, *26* (9), 1473−1524.
(66) Iovleva, M. M. Schematic phase-diagram of the cellulose - N-methylmorpholine-N-oxide monohydrate system. *Polym. Sci. U.S.S.R.* **1989**, *31* (4), 808−812.
(67) Biganska, O.; Navard, P.; Bedue, O. Crystallisation of cellulose/N-methylmorpholine-N-oxide hydrate solutions. *Polymer* **2002**, *43* (23), 6139−6145.
(68) Maia, E.; Peguy, A.; Perez, S. Cellulose organic-solvents 0.1. The structures of anhydrous N-methylmorpholine N-oxide and N-methylmorpholine N-oxide monohydrate. *Acta Crystallogr., Sect. B: Struct. Crystallogr. Cryst. Chem.* **1981**, *37* (OCT), 1858−1862.
(69) Rosenau, T.; Hofinger, A.; Potthast, A.; Kosma, P. On the conformation of the cellulose solvent N-methylmorpholine-N-oxide (NMMO) in solution. *Polymer* **2003**, *44* (20), 6153−6158.
(70) Kast, K. M.; Reiling, S.; Brickmann, J. Ab initio investigations of hydrogen bonding in aliphatic N-oxide-water systems. *J. Mol. Struct.: THEOCHEM* **1998**, *453*, 169−180.
(71) Livingston, N. J.; Spittlehouse, D. L. Carbon isotope fractionation in tree ring early and late wood in relation to intra-growing season water balance. *Plant, Cell Environ.* **1996**, *19* (6), 768−774.
(72) Oberhuber, W.; Gruber, A. Climatic influences on intra-annual stem radial increment of Pinus sylvestris (L.) exposed to drought. *Trees* **2010**, *24* (5), 887−898.
(73) Zweifel, R.; Zimmermann, L.; Zeugin, F.; Newbery, D. M. Intra-annual radial growth and water relations of trees: implications towards a growth mechanism. *J. Exp. Bot.* **2006**, *57* (6), 1445−1459.
(74) Potter, S. L.; Chan, M. A. Joint controlled fluid flow patterns and iron mass transfer in Jurassic Navajo Sandstone, Southern Utah, USA. *Geofluids* **2011**, *11* (2), 184−198.
(75) Mitra, M. K.; Muthukumar, M. Theory of spinodal decomposition assisted crystallization in binary mixtures. *J. Chem. Phys.* **2010**, *132* (18), 184908.
(76) Pohjanlehto, H.; Setälä, H. M.; Kiely, D. E.; McDonald, A. G. Lignin-xylaric acid-polyurethane-based polymer network systems: Preparation and characterization. *J. Appl. Polym. Sci.* **2014**, *131* (1), 39714.

DOI: 10.1021/acs.biomac.5b00977
Biomacromolecules XXXX, XXX, XXX−XXX